J. Biochem. **135**, 487–494 (2004)
DOI: 10.1093/jb/mvh056

Mass Spectrometry of Hydrogen/Deuterium Exchange of *Escherichia coli* Dihydrofolate Reductase: Effects of Loop Mutations

Tatsuya Yamamoto, Shunsuke Izumi, Eiji Ohmae and Kunihiko Gekko*

Department of Mathematical and Life Sciences, Graduate School of Science, Hiroshima University, Higashi-Hiroshima 739-8526

Received December 5, 2003; accepted February 6, 2004

To address the effects of single amino acid substitutions on the structural fluctuation of *Escherichia coli* dihydrofolate reductase (DHFR), hydrogen/deuterium exchange kinetics were investigated at 15°C with wild-type and mutant DHFRs at Gly67 (six mutants) and Gly121 (eight mutants) located in two flexible loops, by means of electrospray ionization mass spectrometry. These mutations induced significant changes in the first-order rate constant of proton exchange, k_{ex} (0.10–0.27 min^{-1}), the number of fast-exchangeable protons, ΔM_0 (164–222 Da), and the number of protons protected from exchange, ΔM_∞ (15–56 Da), relative to the corresponding values for the wild-type enzyme (k_{ex} = 0.18 min^{-1}, ΔM_0 = 164 Da, and ΔM_∞ = 50.5 Da). These kinetic parameters were strongly correlated with the volume of introduced amino acids, but partly correlated with adiabatic compressibility (volume fluctuation), stability, and enzymatic activity. These results indicate that the local structure change due to a single amino acid substitution in loop regions is dramatically magnified to affect the structural fluctuation of the whole DHFR molecule, resulting in complicated changes in its stability and function.

Key words: dihydrofolate reductase, H/D exchange, loop mutation, mass spectrometry, structural fluctuation.

Abbreviations: DHFR, dihydrofolate reductase; ESI-MS, electrospray ionization mass spectrometry; H/D, hydrogen/deuterium; MALDI-MS, matrix-assisted laser desorption/ionization mass spectrometry.

How does a single amino acid substitution in a protein affect the fluctuation of its structure? This is a basic issue for understanding the structure–function relationships of enzymes, but information in this area is limited despite many studies involving mutants. Among various experimental techniques for detecting protein dynamics (*1–4*), hydrogen/deuterium (H/D) exchange is a novel means of determining concomitantly the exchange rate and the number of protons involved (*5*, *6*). H/D exchange has been monitored mainly by infrared spectroscopy and NMR (*7–9*), but the recent development of electrospray ionization mass spectrometry (ESI-MS) and matrix-assisted laser desorption/ionization mass spectrometry (MALDI-MS) has opened a new field in the study of H/D exchange in proteins, because the number of exchangeable protons can be determined rapidly and with an accuracy of 1.006 Da using only a small sample. Zhang and Smith were the first to show the usefulness of mass spectrometry coupled with pepsin digestion in the study of H/D exchange of proteins (*10*). This technique has been applied to studies on protein–inhibitor interactions (*11*) and conformational changes (*12–14*). We recently determined a backbone-flexibility map of *Escherichia coli* dihydrofolate reductase (DHFR) by MALDI-MS coupled with H/D exchange and pepsin digestion (*15*). However, there have been few reports on mutation effects (*16*).

DHFR from *E. coli* is excellent for studying the structure–fluctuation–function relationships of enzymes. It is a monomeric protein consisting of 159 amino acids with no disulfide bonds, and catalyzes the NADPH-linked reduction of dihydrofolate to tetrahydrofolate. As shown in Fig. 1, DHFR has several loops comprising residues 9–24, 64–72, 117–131, and 142–149, as revealed by the large B-factor in the X-ray crystal structure (*17*, *18*). The movie constructed by Sawaya and Kraut (*18*) demonstrated how the loops of DHFR actively and cooperatively move to accommodate the coenzyme and substrate. In previous studies (*19–21*), we found that site-direct mutagenesis at Gly67, Gly121, and Ala145 in three loops significantly influences the stability and function of this enzyme, even though these positions are far away from the catalytic residue Asp27. Interestingly, double mutants at Gly67 and Gly121, whose α-carbons are mutually separated by 27.7 Å, have nonadditive effects on the stability and function (*22*). These results suggest that the mutations alter the structural fluctuation of the entire protein molecule and that a systematic study on the fluctuation of the mutants would reveal how a single amino acid substitution is linked to the fluctuation of this enzyme.

From this viewpoint, we used ESI-MS to study the H/D exchange kinetics of wild-type DHFR and several DHFR mutants as to two sites: Gly67 (six mutants) and Gly121 (eight mutants). Based on the correlation of the H/D exchange kinetic parameters with the type of introduced amino acid, adiabatic compressibility, stability, and enzy-

*To whom correspondence should be addressed. Fax: +81-82-424-7387; E-mail: gekko@sci.hiroshima-u.ac.jp

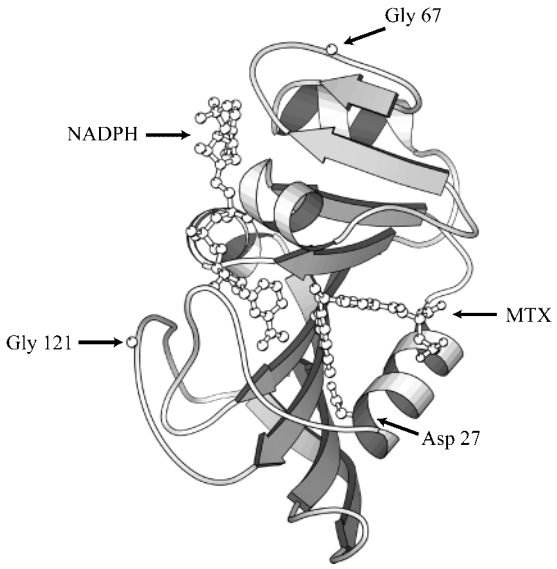

Fig. 1. **The structure of a DHFR–MTX–NADPH ternary complex (PDBID:1rx3) (*18*).** Positions Gly67, Gly121, and Asp27 (a catalytic site residue) are indicated. This figure was produced using the graphics program Molscript (*33*).

matic activity, the effects of mutations on the structural fluctuation of this enzyme are discussed focusing on the role of the loops. To our knowledge, this is the first systematic mass spectrometry investigation on the H/D exchange of a protein containing loop mutations.

MATERIALS AND METHODS

Materials—All mutant DHFR genes were prepared with overexpression plasmids pTP64-1 (5.3 kb) and pTZwt1-3 (3.7 kb) (*23*). The oligonucleotides used for site-directed mutagenesis and the details of mutant construction are given elsewhere (*19*, *20*). The wild-type and all mutant DHFRs obtained from *E. coli* strain HB101 were purified on a methotrexate-agarose affinity column. The DHFRs were fully dialyzed against 10 mM phosphate buffer (pH 7.0) containing 0.1 mM EDTA and 0.1 mM dithiothreitol at 4°C. For mass spectrometry, the DHFR solutions were finally dialyzed against 1 mM ammonium acetate (pH 7.1). The concentrations of DHFRs were determined by absorption measurement with a spectrophotometer (V-560, JASCO). A molar extinction coefficient of 31,100 $M^{-1}\cdot cm^{-1}$ at 280 nm was used for the wild-type DHFR (*24*). For the mutants, this coefficient was corrected using the molecular weights and chromophores of the amino acids introduced. The characteristics of the mutants used are presented in Table 1.

D_2O (99.9 atom % D) and acetic acid-*d* (99 atom % D) were purchased from EURISO-TOP and IsoTec (USA), respectively. All other chemicals were of analytical grade.

H/D Exchange—H/D exchange was initiated by mixing 400 μl of D_2O with 40 μl aliquots of 0.2–0.5 mM DHFR stock solutions (1 mM ammonium acetate, pH 7.1) in capped 1.5-ml centrifuge tubes at 15°C. No correction was made for the difference in pH between H_2O and D_2O. After a certain interval (1 min in most cases), 8 μl of the reaction mixture was removed and the H/D exchange reaction was quenched by adding 2 μl of 20% acetic acid (H:D = 1:10, pH 2.5); this mixture was then injected immediately into a mass spectrometer to determine the molecular weight of the protein as a function of time over 50 min. The quenching time was defined as the H/D exchange time, *t*. Since the deuterium concentration in the solution was very high under the experimental conditions used (H:D = 1:10), the H/D exchange of each amide proton followed first-order kinetics at a constant pH and temperature (*25*). Therefore, the time course of H/D exchange was analyzed using the following equation:

$$M_t = M_\infty - A \exp(-k_{ex}t) \quad (1)$$

where M_t and M_∞ are the molecular weights at the exchange time of t and infinity, respectively; A is the number of exchangeable protons that can be detected during the exchange time; and k_{ex} is the apparent first-order rate constant of H/D exchange. The recorded k_{ex}

Table 1. **Characteristics of the wild-type and mutant DHFRs.**[a]

	V (Å^3)	$\Delta g_{tr}°$ (kJ·mol^{-1})	$\Delta G°$ (kJ·mol^{-1})	m (kJ·mol^{-1} · M^{-1})	K_m (μM)	k_{cat} (s^{-1})	k_{cat}/K_m ($\mu M^{-1}\cdot s^{-1}$)	$\beta_s°$ (Mbar^{-1})
Wild type	48	0	25.4	–8.19	1.3	24.6	18.9	1.7
G67A	67	2.1	27.6	–9.78	1.1	20.0	18.2	–0.1
G67V	105	6.3	21.5	–7.44	1.3	19.1	14.7	1.1
G67S	73	–1.3	25.7	–9.11	1.4	26.4	18.9	1.9
G67T	93	1.7	24.5	–9.36	1.8	26.6	14.8	1.4
G67C	86	4.2	23.9	–8.57	1.2	24.6	20.5	1.7
G67D	91	–10.5	24.8	–9.49	1.2	20.6	17.2	3.0
G121A	67	2.1	27.5	–9.61	2.7	8.5	3.1	–0.4
G121V	105	6.3	21.3	–8.03	1.4	0.94	0.67	3.7
G121L	124	7.5	22.8	–8.19	2.3	0.94	0.41	–
G121Y	141	9.6	24.6	–9.03	2.5	4.4	1.8	–0.7
G121S	73	–1.3	25.5	–8.40	1.8	5.2	2.9	0.7
G121C	86	4.2	25.8	–9.03	1.5	8.4	5.6	5.5
G121F	135	10.5	–	–	–	–	–	–
G121H	118	2.1	25.0	–9.45	2.2	4.8	2.2	–1.8

[a]V and $\Delta g_{tr}°$ are the van der Waals volume and hydrophobicity of amino acid residues introduced, respectively (*4*). $\Delta G°$ and m are the Gibbs free energy change and cooperativity of unfolding by urea, respectively (*19*, *20*). K_m and k_{cat} represent the Michaelis constant and rate constant of enzyme catalysis, respectively (*19*, *20*). $\beta_s°$ represents the adiabatic compressibility in solution (*31*).

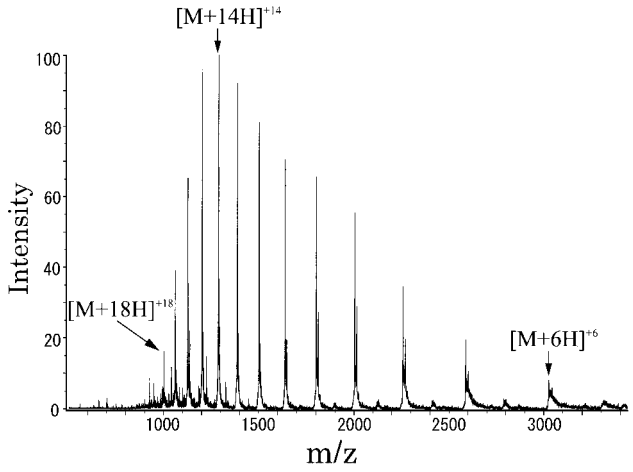

Fig. 2. **ESI mass spectrum of the wild-type DHFR.** The spectrum was measured in 1 mM ammonium actate (pH 7.1) and at the vaporizing temperature of 180°C.

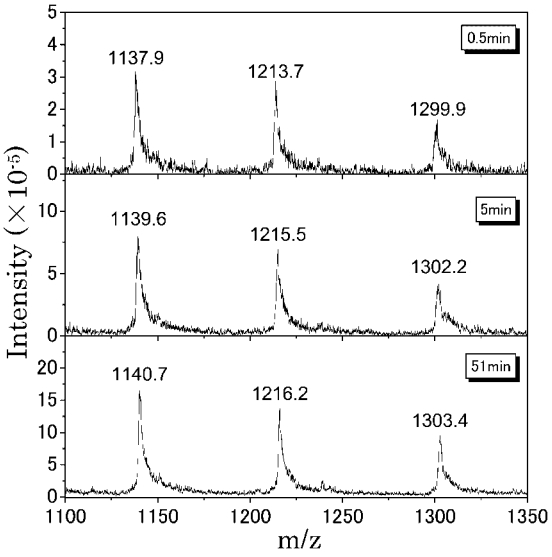

Fig. 3. **ESI mass spectra of the wild-type DHFR with $[M+nH]^{+n}$ ions (n = +14, +15, and +16) at 0.5 min (top), 5 min (middle), and 51 min (bottom) after initiation of H/D exchange in D_2O.**

value represents the mean of the exchange rates of different amide, side-chain, and terminal-residue protons.

Mass Spectrometry—The H/D exchange time course for DHFRs was examined with an electrospray ionization mass spectrometer (JMS-SX 102A JEOL) equipped with an electrospray ion source (ESI10HS). Proteins were introduced into the electrospray ionization source at the rate of 0.2 ml·min^{-1} using a liquid chromatography pump. Protein ions were generated by ESI at a needle voltage of 2000 V, and accelerated in the positive mode at 5,000 V. The temperature of the vaporizer was set to 180°C. The orifice, ring-electrode, and ion-guide voltages were 50, 150, and 4 V, respectively. The pressure in the analyzer was approximately 1×10^{-3} Pa.

RESULTS

Mass Spectra of Wild-Type DHFR—Figure 2 shows an ESI mass spectrum of the wild-type DHFR in 1 mM ammonium acetate (pH 7.1). The positive charge of the protein is distributed in the range of +8 to +21, being centered at +16. This charge profile appears to be a mixture of two distributions. The two distributions were more clearly observed when the protein was ionized in water (pH 6.3) and at the low vaporization temperature of 25°C (data not shown), suggesting that these different ionization states are not caused by denaturation of the protein but are due to the native form. Figure 3 shows mass spectra of the wild-type DHFR with positive charges of +14, +15, and +16 at 0.5, 5, and 51 min after mixing the DHFR solution with D_2O. All peaks shift to a larger m/z value and the peak width becomes narrower over time. Similar results were obtained for all the mutant DHFRs. In this study, we analyzed the H/D exchange kinetics using the smallest centroid masses of the isotopic envelopes in the respective charge peaks of +14, +15, and +16 to eliminate the effects of the adducts of other small molecules. From the mass spectra, it was confirmed that the cysteine residues of none of the mutants were oxidized during the sample preparation. The H/D exchange did not influence the conformation of DHFR, as monitored with circular dichroism spectra (data not shown).

H/D Exchange Kinetics—Figure 4 plots the molecular weights of the wild-type and mutant DHFRs as a function of the H/D exchange time. The maximum incorporation of deuterium occurs within 50 min under the conditions used. It should be noted that all these time courses refer to the exchange of amide protons, because all the side-chain protons should be perfectly exchanged at the time of quenching of the H/D exchange reaction with acetic acid (pH 2.5). The observed time course appears to follow an exponential curve, although a large part of the fast phase cannot be detected. The least-squares regression lines calculated with Eq. 1 fit the data points satisfactorily, as also confirmed by residual-plot analysis (data not shown). Therefore, the H/D exchange of all proteins follows first-order reaction kinetics. The kinetic parameters calculated (M_∞, A, and k_{ex}) are listed in Table 2. The difference between M_∞ and A, which is defined as M_0 (= $M_\infty - A$), is also listed in Table 2. The molecular weight, M_w, of each mutant in H_2O and the theoretical molecular weight for maximum deuterium incorporation, M_∞^{theo}, at an H/D ratio of 1:10 are listed in the second and third columns of Table 1, respectively. The difference between M_0 and M_w, ΔM_0 (= $M_0 - M_w$), refers to the number of fast exchangeable protons exchanged by t = 0, with most of the side-chain protons being involved in this fast phase. The difference between M_∞^{theo} and M_∞, ΔM_∞ (= $M_\infty^{theo} - M_\infty$), indicates the number of amide protons protected from deuterium exchange at $t = \infty$. The values of ΔM_0 and ΔM_∞ are also listed in Table 2.

Evidently, each mutant shows significant changes in k_{ex} (0.10–0.27 min^{-1}), ΔM_0 (164–222 Da), and ΔM_∞ (15–56 Da) relative to the corresponding values for the wild-type enzyme (k_{ex} = 0.18 min^{-1}, ΔM_0 = 164 Da, and ΔM_∞ = 50.5 Da). These results indicate that the structural fluctuation of the DHFR molecule is significantly influenced by

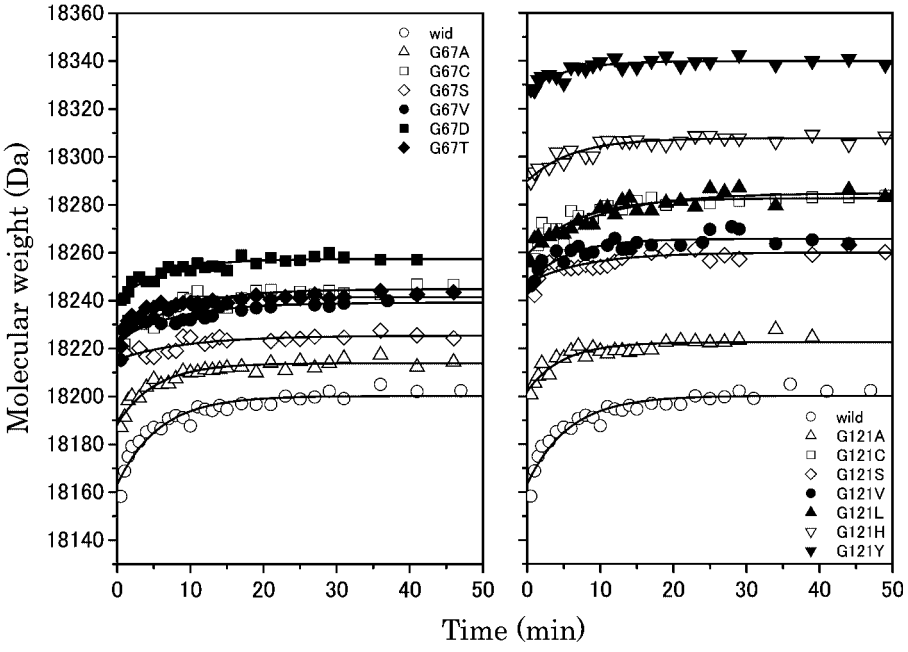

Fig. 4. **Plots of molecular weights of the wild-type and mutant DHFRs at sites 67 and 121 against the H/D exchange time.**

single amino acid substitutions in two flexible loops far from the active site.

DISCUSSION

Mass Spectrum and H/D Exchange of Wild-Type DHFR—Figure 2 suggests that the mass spectrum of the wild-type DHFR consists of two charge distributions that are caused by different conformations in the native state. There is considerable experimental evidence that DHFR has two stable conformations with different affinities for the cofactor, substrate, and inhibitor in enzymatic kinetics (*26*, *27*). Refolding kinetics follow a complicated mechanism involving several conformations in the native and denatured states (*28*). X-ray analysis also indicates a variety of conformations in the crystal that are classified into three major conformations – "open," "closed," and "occluded"–associated with the Met20 loop (*18*). The equilibrium between the "open" and "closed" conformers in solution has been confirmed by NMR (*28*, *29*). At present, it is unknown whether or not these coexisting conformers are ionized with different charges, but if this is the case, the "open" conformer should be more susceptible to ionization than the "closed" one. It is then likely that the peaks centered at +16 and around +10 arise from the "open" and "closed" conformers, respectively. The exchange rate between the "open" and "closed" conformers of wild-type apo-DHFR is approximately 35 s^{-1} (*29*), which is faster than the exchange rate of the exposed protons in solution (~15 s^{-1}) (*30*), and so the H/D exchange properties observed using the +14, +15, and +16 peaks can be largely ascribed to the "open" conformer of the

Table 2. **H/D exchange parameters of the wild-type and mutant DHFRs at sites 67 and 121.**[a]

Mutant	M_w (Da)	M_∞^{theo} (Da)	M_0 (Da)	M_∞ (Da)	k_{ex} (min^{-1})	ΔM_0 (Da)	A (Da)	ΔM_∞ (Da)
Wild type	17,999.2	18,250.7	18,163.4	18,200.2 ± 1.0	0.18 ± 0.02	164.3	36.8 ± 2.2	50.5
G67A	18,013.2	18,264.7	18,188.3	18,213.9 ± 0.7	0.20 ± 0.03	175.1	25.6 ± 1.5	50.9
G67V	18,041.3	18,292.8	18,223.4	18,239.2 ± 1.3	0.12 ± 0.04	182.2	15.8 ± 2.0	53.6
G67S	18,029.2	18,281.7	18,215.5	18,225.4 ± 0.9	0.10 ± 0.03	186.3	10.0 ± 1.3	56.2
G67T	18,043.2	18,295.7	18,223.1	18,241.5 ± 0.5	0.27 ± 0.05	179.9	18.4 ± 1.7	54.2
G67C	18,045.3	18,297.7	18,221.4	18,244.8 ± 1.1	0.13 ± 0.03	176.1	23.4 ± 1.9	52.9
G67D	18,057.2	18,309.7	18,240.3	18,257.4 ± 0.6	0.16 ± 0.03	183.1	17.2 ± 1.2	52.2
G121A	18,013.2	18,264.7	18,202.2	18,222.5 ± 0.9	0.21 ± 0.05	189.0	20.4 ± 2.0	42.2
G121V	18,041.3	18,292.8	18,246.9	18,265.7 ± 1.0	0.19 ± 0.05	205.7	18.8 ± 2.2	27.1
G121L	18,055.3	18,306.8	18,259.4	18,284.8 ± 1.5	0.10 ± 0.02	204.2	25.4 ± 1.9	22.0
G121Y	18,105.3	18,357.7	18,327.4	18,339.9 ± 0.6	0.19 ± 0.05	222.1	12.5 ± 1.4	17.8
G121S	18,029.2	18,281.7	18,247.1	18,260.0 ± 1.2	0.13 ± 0.05	217.9	12.9 ± 2.1	21.7
G121C	18,045.3	18,297.7	18,259.2	18,282.7 ± 1.4	0.14 ± 0.03	213.9	23.5 ± 2.6	15.0
G121F	18,089.3	18,340.8	18,304.2	18,322.1 ± 1.2	0.18 ± 0.05	214.9	17.9 ± 2.4	18.8
G121H	18,079.3	18,331.7	18,289.8	18,307.7 ± 0.7	0.17 ± 0.03	210.5	17.9 ± 1.4	24.0

[a] M_w is the molecular weight of DHFR in H_2O, M_∞^{theo} is the theoretical molecular weight for maximum deuterium incorporation in D_2O, M_0 is the molecular weight at $t = 0$, and M_∞ is the molecular weight at $t = \infty$. The molecular weight differences are defined as $\Delta M_0 = (M_0 - M_w)$ and $\Delta M_\infty = (M_\infty^{theo} - M_\infty)$. k_{ex} is the apparent first-order rate constant of H/D exchange.

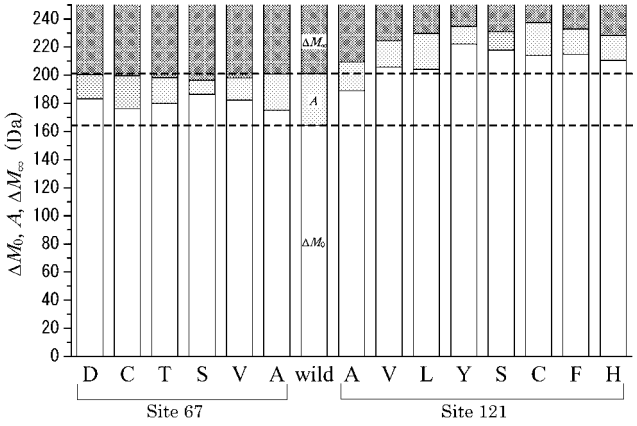

Fig. 5. **H/D exchange mass profiles of the wild-type and mutant DHFRs at sites 67 and 121. White, ΔM_0; light gray, A; dark gray, ΔM_∞. Broken lines represent the mass level of the wild-type DHFR.**

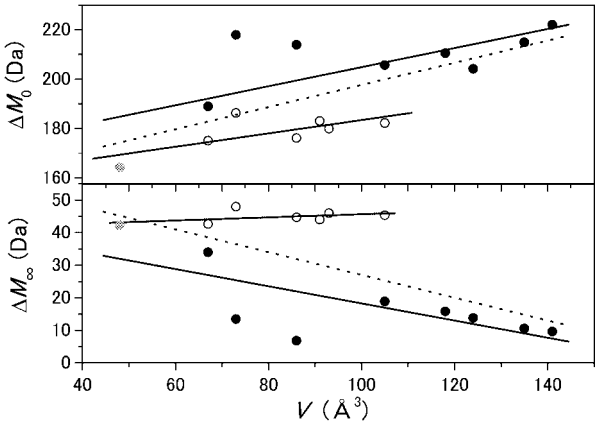

Fig. 6. **Plots of ΔM_0 and ΔM_∞ against the van der Waals volume (V) of amino acid residues introduced at sites 67 (open circles) and 121 (closed circles).** Gray circles are for the wild-type DHFR. Solid lines represent the least-squares linear regression for each data set at sites 67 and 121. The least-squares linear regression for all data points at sites 67 and 121 are shown by dotted lines.

Met20 loop. However, our preliminary experiment indicated that the H/D exchange kinetic parameters (k and M_∞) obtained from the peaks of +10 to +8 are consistent with those obtained from the +14, +15, and +16 peaks within experimental error. Therefore, the observed H/D exchange properties would mainly reflect the structural fluctuation of the whole DHFR molecule in the native form and thus would be useful for evaluating the effects of mutation on the fluctuation.

Effects of Mutation on H/D Exchange Kinetics—A very characteristic advantage of mass spectrometry is that it can be used to directly determine the number of exchangeable protons. As shown in Table 2, single amino acid substitutions clearly affect the H/D exchange kinetic parameters of DHFR. For easy comparison, the mass difference, ΔM_0, A, and ΔM_∞, of the wild-type and mutant DHFRs at sites 67 and 121 are indicated by bars in Fig. 5. For the wild-type DHFR, 164 (ΔM_0) of 251 total exchangeable protons ($M_\infty^{\text{theo}} - M_w$)—comprising 135 amide protons, 113 side-chain protons, and 3 terminal-residue protons—have already finished being exchanged at $t = 0$. The number of protons protected from exchange (ΔM_∞) is 51, so we can observe mass changes in only 37 of them (about 27% of the total amide protons) within the time range of our experiment. Thus, mass spectrometry has limited applicability for fast H/D exchange processes, but we can detect some characteristic differences in the H/D exchange properties of DHFR mutants.

As shown in Fig. 5, the ΔM_0 values of all mutants are larger than that of the wild-type DHFR, the extent being significant at site 121 compared with at site 67. This suggests that mutations at both sites contribute to enhancement of the fluctuation of the residues on the molecular surface or in flexible regions. On the other hand, ΔM_∞ is hardly affected by mutation at site 67, but is greatly decreased by mutation at site 121. This indicates that the effect of mutation at site 121 extends to the internal residues of the protein molecule or the secondary structures that are not relaxed by mutation at site 67. In a previous H/D exchange study coupled with pepsin digestion of wild-type DHFR (*15*), we found that amide protons in α-helices are easily exchanged with deuterium, and that most of the ΔM_∞ value is attributable to amide protons in β-strands. Therefore, we expect that the β-sheet is partly relaxed to make its amide protons susceptible to H/D exchange on mutation at site 121. The large variations in the ΔM_0 and ΔM_∞ values of mutants at site 121 compared

Table 3. **Correlation coefficients (r) of H/D exchange kinetic parameters for the properties of amino acids introduced (V and Δg_{tr}°), stability (ΔG° and m), function (K_m, k_{cat}, and k_{cat}/K_m), and compressibility (β_s°) of DHFR mutants at sites 67 and 121.**

Kinetic parameter	Mutation site	V	Δg_{tr}°	ΔG°	m	K_m	k_{cat}	k_{cat}/K_m	β_s°
ΔM_0	67	0.71	–0.21	–0.27	–0.20	0.20	–0.07	–0.36	0.26
	121	0.70	0.46	–0.22	–0.19	0.27	–0.81	–0.80	–0.03
	Total	0.65	0.44	–0.14	0.03	0.55	–0.85	–0.86	–0.03
ΔM_∞	67	0.47	0.08	–0.31	0.02	0.53	0.46	–0.21	0.24
	121	–0.72	–0.53	0.31	0.06	–0.11	0.74	0.69	–0.17
	Total	–0.58	–0.51	0.11	–0.09	–0.54	0.91	0.89	–0.03
A	67	–0.69	0.13	0.29	0.14	–0.27	–0.01	0.36	–0.22
	121	–0.54	–0.28	0.05	0.33	–0.46	0.75	0.80	0.34
	Total	–0.44	0.02	0.14	0.11	–0.22	0.16	0.23	0.17
k_{ex}	67	–0.04	–0.04	0.31	–0.48	0.56	0.20	–0.42	–0.25
	121	0.04	0.13	0.24	–0.42	0.18	0.24	0.14	–0.32
	Total	–0.02	0.02	0.27	–0.49	0.19	0.14	0.01	–0.22

with those at site 67 are consistent with the finding that other properties such as enzyme function and compressibility are greatly influenced by mutation at site 121 (Table 1).

Evidently, the kinetic parameters of mutants depend on the amino acids introduced at sites 67 and 121. Figure 6 shows typical plots of ΔM_0 and ΔM_∞ against the van der Waals volume (V) of amino acid residues introduced at both sites. Positive and negative slopes are evident for ΔM_0 and ΔM_∞, respectively, although the correlation with ΔM_∞ at site 67 may be insignificant due to the changes in ΔM_∞ being so small. The calculated correlation coefficients, r, for linear regression are listed in Table 3. These results indicate that H/D exchange is enhanced when the volume of an amino acid increases at both sites. This is opposite to the compressibility investigation results: adiabatic compressibility (β_s°) or volume fluctuation decreases when the volume of an amino acid increases at both sites (*31*). In fact, the last column of Table 3 shows that there is no definite correlation between β_s° and ΔM_0 (or ΔM_∞). Thus, the conformation susceptible to H/D exchange is not necessarily associated with great fluctuation in volume. This is possible because H/D exchange is derived from solvent accessibility, whereas compressibility is mainly determined by atomic packing or cavities in the interior of the protein molecule, and because H/D exchange is depressed in the secondary structures although they play the role of a dynamic domain in volume fluctuation (*15*, *31*). Computer simulation predicts that Gly67 and Gly121 cannot be replaced by any other amino acids without accompanying movements of the backbone polypeptide chain due to changes in the torsion angles, χ_1 and χ_2, of the side chains, which are directed toward the inside of the protein molecule. Therefore, it is likely that overcrowding of amino acid side chains at sites 67 and 121 affects the atomic packing (compressibility) and motility of the backbone chain (H/D exchange) in different ways *via* long-range interactions.

The coefficients for the correlation between the kinetic parameters and hydrophobicity (Δg_{tr}°) of the introduced amino acid residues are also listed in Table 3. H/D exchange appears to be enhanced with increasing hydrophobicity of amino acid side chains at both sites. This correlation is more evident when the data for Asp and Ser with negative Δg_{tr}° values are eliminated, and is opposite to the expectation that the enhanced hydrophobic interaction would stabilize the native structure so as to inhibit the H/D exchange. Thus, the main effect of mutation at both sites would be due to overcrowding of the bulky side chains overcoming the increased hydrophobic interaction.

As shown in Table 3, the rate constant of H/D exchange, k_{ex}, is not correlated with the V and Δg_{tr}° values of introduced amino acid side chains. This may be partly due to the small variations in k_{ex} between different mutants, although they are greater than experimental error. The H/D exchange kinetics of a protein have been explained by the following local unfolding model (*5*, *6*):

$$\mathrm{N(H)} \underset{k_f}{\overset{k_u}{\rightleftarrows}} \mathrm{O(H)} \overset{k_c}{\rightarrow} \mathrm{O(D)} \rightleftarrows \mathrm{N(D)} \qquad (2)$$

where N represents the folded state of a protein; O is a partially unfolded open state in which the exchangeable protons are exposed to the solvent; and k_u, k_f, and k_c are the rate constants for the individual processes. When $k_c > k_f$, the observed rate of exchange, k_{ex}, is determined by the rate of opening of the protein structure, k_u (EX_1 mechanism). If $k_c < k_f$, the observed rate of exchange is $(k_u/k_f)k_c$, and then k_{ex} is proportional to the equilibrium constant for the local unfolding process (EX_2 mechanism). The H/D exchange of proteins follows an EX_2 mechanism under most conditions, with an EX_1 mechanism only being observed under the conditions where the hydrogen exchange is intrinsically very rapid and no longer rate-limiting (*5*). In a previous paper (*15*), we confirmed that the H/D exchange reaction of wild-type DHFR is dominated by an EX_2 mechanism under our experimental conditions (neutral pH). Since k_c is not dependent on introduced amino acids, the mutation effect on the Gibbs free energy change between folded and open states, $\Delta\Delta G$, can be evaluated from

$$\begin{aligned}\Delta\Delta G &= \Delta G\,(\mathrm{mutant}) - \Delta G\,(\mathrm{wild}) \\ &= -RT \ln [(k_u/k_f)^{\mathrm{mutant}}/(k_u/k_f)^{\mathrm{wild}}]\end{aligned} \qquad (3)$$

From the k_{ex} values, we can calculate that the $\Delta\Delta G$ value ranges from –1.0 (G67T) to 1.4 (G67S, G121L) kJ·mol^{-1} depending on the mutations at both sites. These values are within the difference in Gibbs free energy change of urea denaturation between the wild-type and mutant DHFRs; $\Delta\Delta G^\circ = \Delta G^\circ(\mathrm{mutant}) - \Delta G^\circ(\mathrm{wild}) = -4.2$ to 2.2 kJ·mol^{-1} (Table 1). This suggests that mutations at both sites do not cause as large perturbations in the free energy of a partially unfolded open state as in the urea-unfolded state.

Relationship between H/D Exchange and Stability—The values of the Gibbs free energy change of urea denaturation, ΔG°, and the cooperativity parameter of unfolding, m, of the wild-type and mutant DHFRs are listed in Table 1. Evidently, the structural stability is influenced (in most cases, destabilized) by mutations at sites 67 and 121. As shown in Table 3, however, there is no definite correlation between the H/D exchange properties (ΔM_0, ΔM_∞, and k_{ex}) and stability (ΔG° and m), although the marginally negative correlation between k_{ex} and m suggests fast H/D exchange for mutants unfolding with high cooperativity; thus the conformation resistant to H/D exchange is not necessarily stable. This may be partly attributable to the H/D kinetic parameters of the native state only, whereas ΔG° and m are determined as the differences in the free energy and solvent-accessible surface area of a protein between the native and denatured states. In this regard, it is noticeable that the stability decreases with increasing hydrophobicity of the amino acids introduced at both sites (*i.e.*, reverse hydrophobic effect) (*19*, *20*).

Relationship between H/D Exchange and Function—The steady-state kinetic parameters for the enzyme reactions (K_m and k_{cat}) of the wild-type and mutant DHFRs are listed in Table 1. The K_m value is only slightly influenced by mutation at both sites, whereas k_{cat} changes significantly, especially at site 121, resulting in a great change in enzyme activity (k_{cat}/K_m). This is very interesting because it is unlikely that the mutation sites participate directly in the enzyme reaction: the α-carbons of Gly67 and Gly121 are 29.3 and 19.0 Å from the catalytic

site Asp27, respectively, and are at least 8.5 and 10.6 Å from the NADPH molecule (*18*).

Table 3 lists the correlation coefficients of H/D exchange parameters with K_m, k_{cat}, and k_{cat}/K_m. Although there is no clear correlation between k_{ex} and these enzyme kinetic parameters, ΔM_0 and ΔM_∞ are negatively and positively correlated with k_{cat}/K_m (with the exception of ΔM_∞ at site 67), respectively. A similar correlation is also observed for k_{cat}, although the r value is small for ΔM_0 at site 67. These results suggest that the conformation resistant to H/D exchange is favorable for the enzymatic function predominantly due to the enhanced catalytic reaction rate (k_{cat}). This is contrary to the observation that the enzyme activity increases with increasing compressibility (*31*). This discrepancy is attributable to H/D exchange and compressibility representing opposing measures of structural fluctuation of protein molecules, as described above. Therefore, considerable caution is necessary when evaluating the role of structural fluctuation in enzyme function and structural stability based on H/D exchange parameters.

As revealed by the present study, the H/D exchange properties of DHFR are sensitive to single amino acid substitutions at sites 67 and 121 in the flexible loops, the extent being more significant at site 121. The H/D exchange parameters obtained show a partial correlation with the characteristic properties of the mutants (amino acids introduced, structural stability, compressibility, and enzymatic function). These results support our proposals that DHFR is a highly fluctuating protein and that a mutation-induced small alteration in the local structure in loop regions is dramatically magnified in the overall protein dynamics *via* long-range atomic reconstruction, leading to change in the stability and function (*19–22*, *32*). Mass spectrometry of H/D exchange of ligand–DHFR complexes in progress should provide more detailed information on the structure–fluctuation–function relationship of this enzyme.

We wish to thank Professor Tsutomu Masujima of Hiroshima University for providing the MALDI-MS facilities. We also thank the Instrument Center for Chemical Analysis and the Faculty of Applied Biological Sciences of Hiroshima University for allowing us to use their ESI-BE double-focusing mass spectrometer and ESI-ion-trap-MS/MS, respectively. This work was partly supported by a Grant-in Aid for Scientific Research from the Ministry of Education, Science, Sports and Culture of Japan (No. 10480159).

REFERENCES

1. Karplus, M. and McCammon, J.A. (1981) The internal dynamics of globular proteins. *CRC Crit. Rev. Biochem.* **9**, 293–349
2. Gekko, K. and Hasegawa, Y. (1986) Compressibility-structure relationship of globular proteins. *Biochemistry* **25**, 6563–6571
3. Wüthrich, K. (1990) Structure and dynamics in proteins of pharmacological interest. *Biochem. Pharmacol.* **40**, 55–62
4. Creighton, T. (1993) in *Proteins: Structure and Molecular Properties*, Freeman and Company, New York
5. Hvidt, A. and Nielsen, S.O. (1966) Hydrogen exchange in proteins. *Adv. Protein Chem.* **21**, 287–386
6. Englander, S.W. and Kallenbach, N.R. (1983) Hydrogen exchange and structural dynamics of proteins and nucleic acids. *Q. Rev. Biophys.* **16**, 521–655
7. Nakanishi, M. and Tsuboi, M. (1976) Structure and fluctuation of a *Streptomyces* subtilisin inhibitor. *Biochim. Biophys. Acta* **434**, 365–376
8. Wagner, G. and Wüthrich, K. (1982) Amide proton exchange and surface conformation of the basic pancreatic trypsin inhibitor in solution. Studies with two-dimensional nuclear magnetic resonance. *J. Mol. Biol.* **160**, 343–361
9. Akasaka, K., Inoue, T., Hatano, H., and Woodward, C.K. (1985) Hydrogen exchange kinetics of core peptide protons in *Streptomyces* subtilisin inhibitor. *Biochemistry* **24**, 2973–2979
10. Zhang, Z. and Smith, D.L. (1993) Determination of amide hydrogen exchange by mass spectrometry: a new tool for protein structure elucidation. *Protein Sci.* **2**, 522–531
11. Akashi, S. and Takio, K. (2000) Characterization of the interface structure of enzyme-inhibitor complex by using hydrogen-deuterium exchange and electrospray ionization Fourier transform ion cyclotron resonance mass spectrometry. *Protein Sci.* **9**, 2497–2505
12. Babu, K.R. and Douglas, D.J. (2000) Methanol-induced conformations of myoglobin at pH 4.0. *Biochemistry* **39**, 14702–14710
13. Powell, K.D., Wales, T.E., and Fitzgerald, M.C. (2002) Thermodynamic stability measurements on multimeric proteins using a new H/D exchange- and matrix-assisted laser desorption/ionization (MALDI) mass spectrometry-based method. *Protein Sci.* **11**, 841–851
14. Englander, J.J., Del Mar, C., Li, W., Englander, S.W., Kim, J.S., Stranz, D.D., Hamuro, Y., and Woods V.L., Jr. (2003) Protein structure change studied by hydrogen-deuterium exchange, functional labeling, and mass spectrometry. *Proc. Natl Acad. Sci. USA* **100**, 7057–7062
15. Yamamoto, T., Izumi, S., and Gekko, K. (2004) Mass spectrometry on segment-specific hydrogen exchange of dihydrofolate reductase. *J. Biochem.* **135**, 17–24
16. Wang, F., Li, W., Emmett, M.R., Hendrickson, C.L., Marshall, A.G., Zhang Y.L., Wu, L., and Zhang, Z.Y. (1998) Conformational and dynamic changes of *Yersinia* protein tyrosine phosphatase induced by ligand binding and active site mutation and revealed by H/D exchange and electrospray ionization Fourier transform ion cyclotron resonance mass spectrometry. *Biochemistry* **37**, 15289–15299
17. Bystroff, C. and Kraut, J. (1991) Crystal structure of unliganded *Escherichia coli* dihydrofolate reductase: Ligand-induced conformational change and cooperativity in binding. *Biochemistry* **30**, 2227–2239
18. Sawaya, M.R. and Kraut, J. (1997) Loop and subdomain movements in the mechanism of *Escherichia coli* dihydrofolate reductase: crystallographic evidence. *Biochemistry* **36**, 586–603
19. Gekko, K., Kunori, Y., Takeuchi, H., Ichihara, S., and Kodama, M. (1994) Point mutations at glycine-121 of *Escherichia coli* dihydrofolate reductase: important roles of a flexible loop in the stability and function. *J. Biochem.* **116**, 34–41
20. Ohmae, E., Iriyama, K., Ichihara, S., and Gekko, K. (1996) Effects of point mutations at the flexible loop glycine-67 of *Escherichia coli* dihydrofolate reductase on its stability and function. *J. Biochem.* **119**, 703–710
21. Ohmae, E., Ishimura, K., Iwakura, M., and Gekko, K. (1998) Effects of point mutations at the flexible loop alanine-145 of *Escherichia coli* dihydrofolate reductase on its stability and function. *J. Biochem.* **123**, 839–846
22. Ohmae, E., Iriyama, K., Ichihara, S., and Gekko, K. (1998) Nonadditive effects of double mutations at the flexible loops, glycine-67 and glycine-121, of *Escherichia coli* dihydrofolate reductase on its stability and function. *J. Biochem.* **123**, 33–41
23. Iwakura, M., Jones, B.E., Luo, J., and Matthews, C.R. (1995) A strategy for testing the suitability of cysteine replacements in dihydrofolate reductase from *Escherichia coli*. *J. Biochem.* **117**, 480–488
24. Fierke, C.A., Johnson, K.A., and Benkovic, S.J. (1987) Construction and evaluation of the kinetic scheme associated with dihydrofolate reductase from *Escherichia coli*. *Biochemistry* **26**, 4085–4092

25. Englander, S.W. and Kallenbach, N.R. (1983) Hydrogen exchange and structural dynamics of proteins and nucleic acids. *Q. Rev. Biophys.* **16**, 521–655
26. Birdsall, B., Feeney, S.J.B., Tendler, S.J., Hammond, D.J., and Roberts, G.C.K. (1989) Dihydrofolate reductase: multiple conformations and alternative modes of substrate binding. *Biochemistry* **28**, 2297–2305
27. Falzone, C.J., Wright, P.E., and Benkovic, S.J. (1991) Evidence for two interconverting protein isomers in the methotrexate complex of dihydrofolate reductase from *Escherichia coli*. *Biochemistry* **30**, 2184–2191
28. Kitahara, R., Sareth, S., Yamada, H., Ohmae, E., Gekko, K., and Akasaka, K. (2000) High pressure NMR reveals active-site hinge motion of folate-bound *Escherichia coli* dihydrofolate reductase. *Biochemistry* **39**, 12789–12795
29. Falzone C.J., Wright P.E., and Benkovic S.J (1994) Dynamics of a flexible loop in dihydrofolate reductase from *Escherichia coli* and its implication for catalysis. *Biochemistry* **33**, 439–442
30. Takahashi, T., Nakanishi, M., and Tsuboi, M. (1978) Hydrogen–deuterium exchange rate between a peptide group and an aqueous solvent as determined by a stopped flow ultraviolet spectrophotometry. *Bull. Chem. Soc. Jpn.* **51**, 1988–1990
31. Gekko, K., Kamiyama, T., Ohmae, E., and Katayanagi, K. (2000) Single amino acid substitutions in flexible loops can induce large compressibility changes in dihydrofolate reductase. *J. Biochem.* **128**, 21–27
32. Cameron, C.E. and Benkovic, S.J. (1997) Evidence for a functional role of the dynamics of glycine-121 of *Escherichia coli* dihydrofolate reductase obtained from kinetic analysis of a site-directed mutant. *Biochemistry* **36**, 15792–15800
33. Kraulis, P.J. (1991) MOLSCRIPT: a program to produce both detailed and schematic plots of protein structures. *J. Appl. Crystallogr.* **24**, 946–950